

Interpreting and Improving Adversarial Robustness of Deep Neural Networks with Neuron Sensitivity

Chongzhi Zhang*, Aishan Liu*, Xianglong Liu**, Yitao Xu, Hang Yu, Yuqing Ma, and Tianlin Li

State Key Laboratory of Software Development Environment, Beihang University,
Beijing, China

{chongzhizhang,xlliu,mayuqing}@nlsde.buaa.edu.cn

{hyu0829,liuaishan,xuyitao}@buaa.edu.cn

litl@act.buaa.edu.cn

Abstract. Deep neural networks (DNNs) are vulnerable to adversarial examples where inputs with imperceptible perturbations mislead DNNs to incorrect results. Despite the potential risk they bring, adversarial examples are also valuable for providing insights into the weakness and blind-spots of DNNs. Thus, the interpretability of a DNN in the adversarial setting aims to explain the rationale behind its decision-making process and makes deeper understanding which results in better practical applications. To address this issue, we try to explain adversarial robustness for deep models from a new perspective of neuron sensitivity which is measured by neuron behavior variation intensity against benign and adversarial examples. In this paper, we first draw the close connection between adversarial robustness and neuron sensitivities, as sensitive neurons make the most non-trivial contributions to model predictions in the adversarial setting. Based on that, we further propose to improve adversarial robustness by constraining the similarities of sensitive neurons between benign and adversarial examples which stabilizes the behaviors of sensitive neurons towards adversarial noises. Moreover, we demonstrate that state-of-the-art adversarial training methods improve model robustness by reducing neuron sensitivities which in turn confirms the strong connections between adversarial robustness and neuron sensitivity as well as the effectiveness of using sensitive neurons to build robust models. Extensive experiments on various datasets demonstrate that our algorithm effectively achieves excellent results.

1 Introduction

Deep Neural Network (DNNs) have demonstrated remarkable performance in a wide spectrum of areas, including computer vision [20,30], speech recognition [28] and natural language processing [5,37]. Despite the significant achievements,

* These authors contributed equally to this work.

** Corresponding author.

unfortunately, the emergence of adversarial examples [4,6,11,12,16,36,38], images containing small perturbations imperceptible to human but extremely misleading to DNNs, casts a cloud over the recent progress of deep learning. Further, adversarial examples also pose potential security threats by attacking or misleading the practical deep learning applications like auto-driving and face recognition system, which may cause pecuniary loss or even people death with severe impairment [21,24,35].

In the past years, plenty of defense methods have been proposed to improve model robustness to adversarial examples, avoiding the potential danger in real world applications. These methods can be roughly categorized into adversarial training [11,22,26], input transformation [8,13,41], elaborately designed model architectures [2,10,17,23,29] and adversarial example detection [25,27,31,44].

Though challenging to deep learning, from another point of view, adversarial examples are also valuable and beneficial for understanding the behaviors of DNNs, which is an extremely difficult problem in the literature due to the myriad of linear and nonlinear operations in the “black-box”. Understanding adversarial examples provides insights into the weaknesses and blind-spots of DNNs in adversarial settings, which in turn offers us clues to interpret and build robust deep learning models. Several studies have been proposed to reveal the “tip of the iceberg” of model robustness towards adversarial noises. Dong *et al.* [7] re-examined the internal representations of DNNs using adversarial examples and further improved their interpretability with an adversarial training scheme. Meanwhile, Xu *et al.* [43] attempted to explore the weakness of models under adversarial conditions by analyzing the effects of different regions within a specific image. More recently, Ilyas *et al.* [15] believed that robust features can be extracted with the help of adversarially robust deep models.

From a high-level perspective, model robustness to noises can be viewed as a kind of global insensitivity property [40]. A deep model is able to learn insensitive representations towards adversarial examples, if it behaves stably without too much performance degeneration when encountering such noises. Thus, by constraining the differences between clean and adversarial pairs in the penultimate or the logit layer of a DNN, several studies have been proposed to defense adversarial examples [18,23]. In contrast to them, this paper tries to uncover the mysteries of model robustness in an adversarial setting from the perspective of behavior sensitivity in a neuron-wise way. By studying neuron behaviors in different layers, we reveal insightful clues for model robustness and weakness from the perspective of neuron sensitivities, which in turn motivate us to introduce a strategy to improve model robustness towards adversarial examples via stabilizing neuron sensitivities.

Our main contributions can be summarized as follows:

- We are the first to demonstrate the concept of *Neuron Sensitivity* that considers the varying intensity of neuron behaviors for adversarial and benign examples, as a criterion to measure the stability of a DNN in adversarial settings.

- Further, we take the first steps to define *Sensitive Neuron*, a set of neurons most sensitive to adversarial examples, which we believe may conduct the most non-trivial contributions to sensitive model behaviors.
- By stabilizing neuron sensitivities towards benign and adversarial examples, we propose the *Sensitive Neuron Stabilizing* (SNS) method to improve model robustness against adversarial noises. Extensive experiments on CIFAR-10 and ImageNet empirically demonstrate that such a simple technique significantly outperforms state-of-the-art adversarial training strategies.
- Empirical studies on neuron sensitivities in different layers of different deep models demonstrate that state-of-the-art adversarial training methods improve model robustness mainly by embedding insensitivity to neurons which in turn confirms the significance of neuron sensitivities towards adversarial robustness.

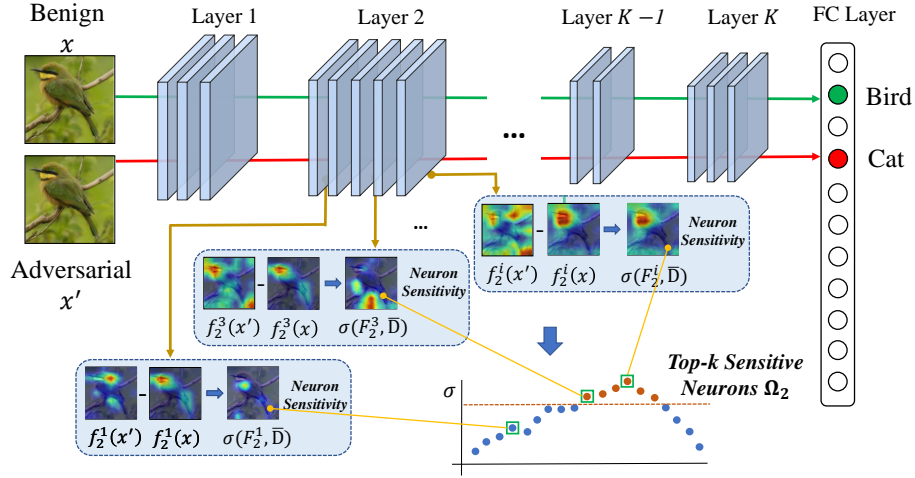


Fig. 1: Our framework of computing *Neuron Sensitivity* and selecting *Sensitive Neurons*. *Neuron Sensitivity* is measured by neuron behavior variation intensities against benign example x and the corresponding adversarial example x' . Neurons with the top- k maximum *Neuron Sensitivity* on specific layers will be selected as *Sensitive Neurons*.

2 Neuron Sensitivity and Sensitive Neuron

Prior studies have shown that different neurons play different roles and possess different importance for model prediction even arranged in the same layer [3, 7, 47]. Inspired by this fact, this section studies the adversarial robustness from the view of neuron behaviors.

Given a dataset \mathbf{D} with data sample $x \in \mathcal{X}$ and label $y \in \mathcal{Y}$, the deep supervised learning model tries to learn a mapping or classification function $F: \mathcal{X} \rightarrow \mathcal{Y}$. The model F consists of L serial layers. For the l -th layer F_l , where

$l = 1, \dots, L$, it contains several neurons, which can also be regarded as a neuron set. We use superscript m to denote the m -th neuron, and satisfying $F_l^m \in F_l$. The output of one neuron F_l^m is equivalent to the m -th channel of the feature map produced by layer l . For model F , this paper chooses the popular deep convolutional neural networks (CNNs) for the visual recognition task.

2.1 Neuron Sensitivity

The model robustness towards noises can be viewed as a global insensitive behavior showing small losses and consistent predictions under noise conditions. Recall the definition of model robustness to noise in [42], which are derived from the idea that if two instances are “similar” then their test errors are close, too:

$$\forall x_i, x_j \in \mathbf{D}, \text{ if } \|x_i - x_j\| < \epsilon \Rightarrow \|\mathcal{L}_F(x_i) - \mathcal{L}_F(x_j)\| \leq e,$$

where x_i and x_j are samples selected randomly from the same dataset \mathbf{D} and $\mathcal{L}_F(\cdot)$ denotes the loss function. $\|\cdot\|$ is a distance metric to quantify the distance between samples and e denotes a small value.

This fact should hold for the benign sample $x \in \mathbf{D}$ from category y and its adversarial example $x' \in \mathbf{D}'$. However, in practice, adversarial examples mislead the non-robust classifier to predict wrong label which is defined as follow:

$$F(x') \neq y \quad \text{s.t.} \quad \|x - x'\| < \epsilon.$$

Intuitively, for a model that owns strong robustness, namely, insensitive to adversarial examples, we expect that the benign sample x and the corresponding adversarial example x' share a similar representation in the hidden layers of the model, leading to similar final predictions as well. Motivated by this intuition, to understand the adversarial robustness of deep models, one can concentrate on the deviation of the feature representation in hidden layers between benign samples and corresponding adversarial examples.

To achieve this goal, we introduce *Neuron Sensitivity* to interpret the model sensitivity from the view of neurons inside it. Specifically, given a benign example x_i , where $i = 1, \dots, N$, from \mathbf{D} and its corresponding adversarial example x'_i from \mathbf{D}' , we can get the dual pair set $\bar{\mathbf{D}} = \{(x_i, x'_i)\}$, and then calculate the neuron sensitivity σ as follow:

$$\sigma(F_l^m, \bar{\mathbf{D}}) = \frac{1}{N} \sum_{i=1}^N \|F_l^m(x_i) - F_l^m(x'_i)\|_1, \quad (1)$$

where $F_l^m(x_i)$ and $F_l^m(x'_i)$ respectively represents outputs of neuron F_l^m towards benign sample x_i and corresponding adversarial example x'_i during the forward process. Here, we use the L_1 norm as the distance metric empirically.

2.2 Sensitive Neuron

Once we have defined *Neuron Sensitivity*, we can further determine the most prominent neurons under this criterion and mark them as the *Sensitive Neuron*

Ω_l as shown below:

$$\Omega_l = \text{top-}k(F_l, \sigma), \quad (2)$$

where $\text{top-}k(\cdot)$ represents top k maximum instances of the input set based on a certain metric, such as neuron sensitivity σ in this case, which means Ω_l is a subset of F_l . This can be easily accomplished by traversing the neurons in each layer and selecting k neurons with the maximal neuron sensitivity according to Equation 1 for N samples.

Obviously, sensitive neurons in each layer correspond to the vulnerable ones in a model towards adversarial examples, where more attention should be paid. Therefore, in the rest of this paper, we mainly focus on understanding the behaviors of sensitive neurons against adversarial examples, so that we can establish connections between neuron sensitivity and model robustness, and further improve the model robustness with sensitive neurons. Figure 1 demonstrates the basic procedure of computing neuron sensitivity and selecting sensitive neurons.

3 Sensitive Neurons and Adversarial Robustness

Apart from viewing DNNs as a black-box from a high-level viewpoint, it is natural for us to treat the model as a white-box and make deeper insights into model adversarial weaknesses from the perspective of sensitive neurons. In this section, we first explore the strong connections between sensitive neurons and adversarial robustness. With several empirical analyses, we surprisingly find that sensitive neurons make the most non-trivial contributions towards model robustness in the adversarial setting. In the following parts of this section, we first illustrate the empirical settings, then give our analyses and discussions.

3.1 Empirical Settings

Datasets and models For empirical analyses, we adopt the widely used **CIFAR-10** and **ImageNet** datasets. CIFAR-10 consists of 60K natural scene color images with 10 classes of size $32 \times 32 \times 3$ [19]. We use VGG-16 [34] and ResNet-18 [14] for CIFAR-10. ImageNet contains 14M images with more than 20k classes [32]. For simplicity, we only choose 200 classes from 1000 in ILSVRC-2012 with 100K and 10k images for training set and test set, respectively. The models we use for ImageNet are VGG-16 and AlexNet [20].

Adversarial attack and defence methods We apply a diverse set of state-of-the-art **adversarial attack methods** including: FGSM [11], Step-LL [22], MI-FGSM [6] and PGD [26]. The implementation details of these attack methods are shown as follows: For FGSM and Step-LL, we set $\epsilon = 8/255$. For MI-FGSM and PGD, we set $\epsilon = 8/255$, step size $\alpha = \epsilon/10$ and iteration $k = 10$. Additionally, the decay factor μ of MI-FGSM is set to 1.0. We choose ℓ_∞ norm to measure the perturbation magnitude for all attack methods.

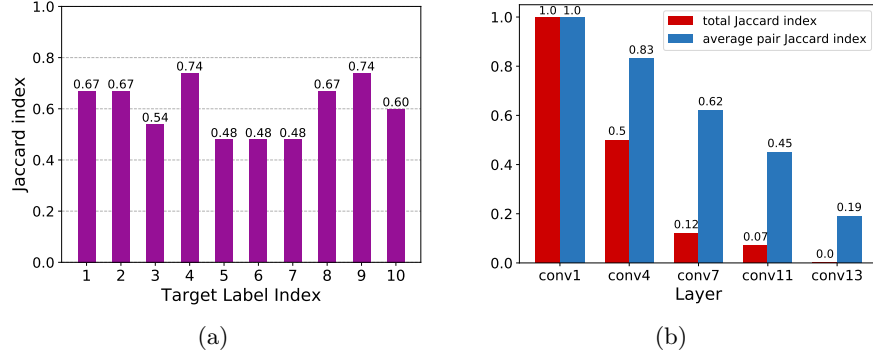


Fig. 2: Neuron similarity of PGD attacked adversarial examples from 10 different target labels with VGG-16 Vanilla model on CIFAR-10. Subfigure (a) shows the Jaccard index of I^y and Ω_{L-1}^y of PGD attack. High similarities between sensitive neurons and important neurons indicate that sensitive neurons uncover the strongest weakness for deep models. Subfigure (b) shows the total Jaccard index and average pair Jaccard index of sensitive neuron sets $\Omega_l^1, \dots, \Omega_l^{10}$. The results indicate that adversarial examples with different target labels tend to share the same flaws of bottom layers, while utilize different fragile neurons in the top layers.

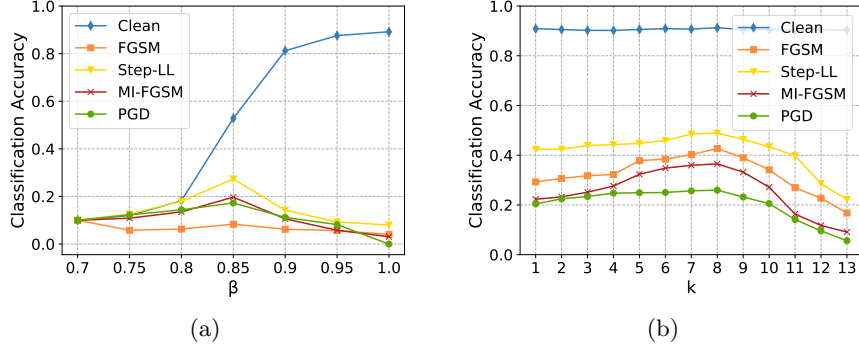


Fig. 3: (a) Sensitive neurons behavior study using suppression coefficient β on CIFAR-10 with VGG-16 Vanilla model. As shown in Subfigure (a), the contrast change of clean accuracy and adversarial accuracy proves the trade-off between adversarial robustness and clean accuracy. Subfigure (b) shows the VGG-16 model trained using Equation 10 on CIFAR-10 when applying top- k layers. SNS training with layers from *conv8* to *conv13* enjoys the strongest model against all kinds of attacks.

As for **adversarial defense models**, we choose the state-of-the-art defense methods including naive adversarial training (NAT) [22], PGD-based adversarial training (PAT) [26], ensemble adversarial training (EAT) [39] and adversarial

logit pairing (ALP) [18]. Among these methods, EAT achieved No.1 in round 1 in *NeurIPS 2017* adversarial defense competition.

3.2 Sensitive Neurons Contribute Most to Model Predictions in Adversarial Setting

We first analyze the behaviors and contributions of sensitive neurons to model robustness in adversarial setting. In order to compute the contribution of neurons towards prediction, we borrow the idea of calculating the contribution from representation of penultimate layer F_{L-1} to logits from [9]: for an input adversarial example x' with predicted class y we can select the important neurons Π by:

$$\Pi^y(x') = \text{top-}k(F_{L-1}, \varphi), \quad (3)$$

where metric $\varphi(F_{L-1}^m, x', y)$ measures the direct contribution from the output of F_{L-1}^m to the logit of target class y . And it can be described as below:

$$\varphi(F_{L-1}^m, x', y) = F_{L-1}^m(x') \cdot W_{my}, \quad (4)$$

where W_{my} is the linear layer mapping from m -th representations to y -th logit. Obviously, the important neurons from penultimate layer denote those units that contribute greatest to the model prediction (target logit) for sample x' .

As important neurons are designed for single adversarial image, we further extend the idea from one adversarial example image to one adversarial example set \mathbf{D}' for a specific target class y :

$$\Gamma^y = \text{top-}k(F_{L-1}, \rho), \quad (5)$$

where metric ρ means the total score of weighted voting by important neurons $\Pi^y(x_1), \dots, \Pi^y(x_N)$ computed with respect to each adversarial image in \mathbf{D}' . Specifically, important neurons for image x_i with higher rank will have larger voting weight. In our experiment, we choose top-20 important neurons for adversarial example set \mathbf{D}' and also select the top-20 sensitive neurons for comparison. For VGG-16 model, we investigate the neurons from *pool5* layer.

Then, we utilize the Jaccard index as the metric to quantify the overlaps and similarities between important neurons and sensitive neurons for the same adversarial example set of a specific target class y from penultimate layer:

$$J(\Omega_{L-1}^y, \Gamma^y) = \frac{|\Omega_{L-1}^y \cap \Gamma^y|}{|\Omega_{L-1}^y \cup \Gamma^y|}, \quad (6)$$

where Ω_{L-1}^y and Γ^y respectively represents the top- k sensitive neuron set and important neuron set for targeted adversarial example set of label y , and the notion $|\cdot|$ denotes the size of set.

As shown in Figure 2 (a), for target labels ranging from 0 to 9, overlap rates of two sets are very high, which indicates that sensitive neurons and important

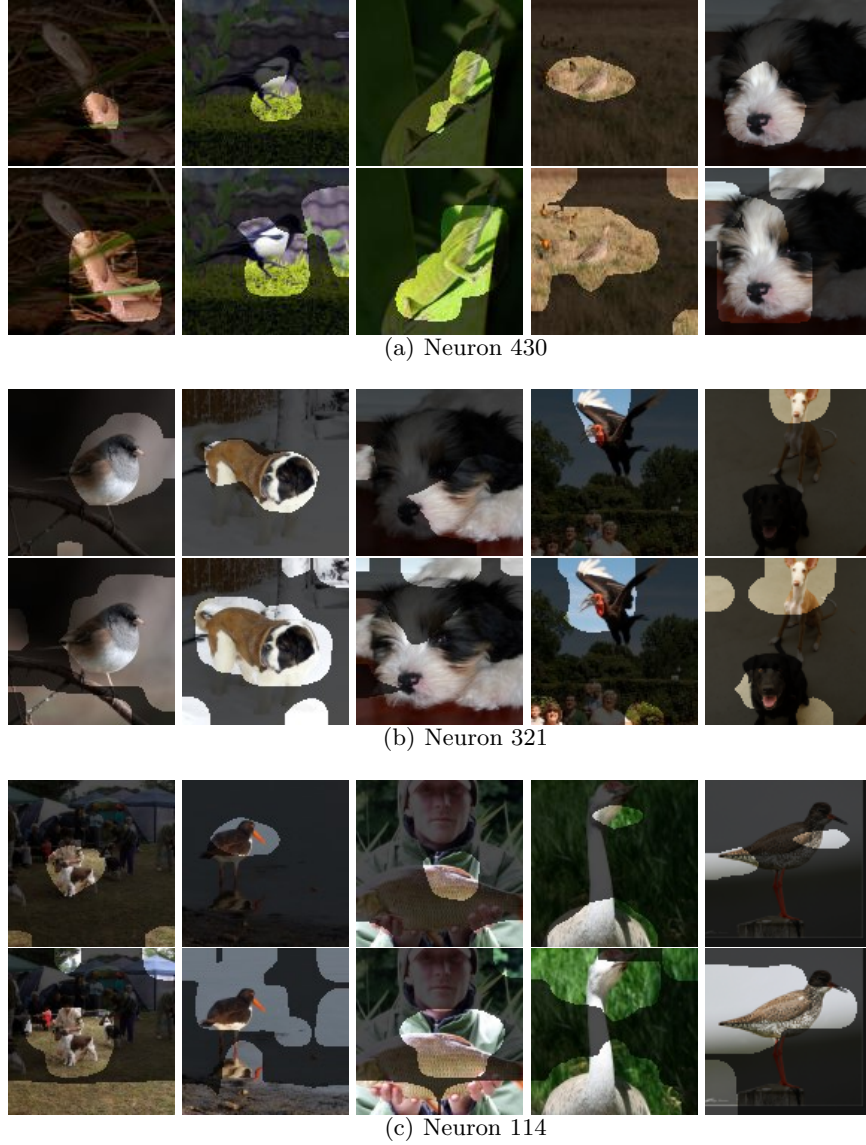
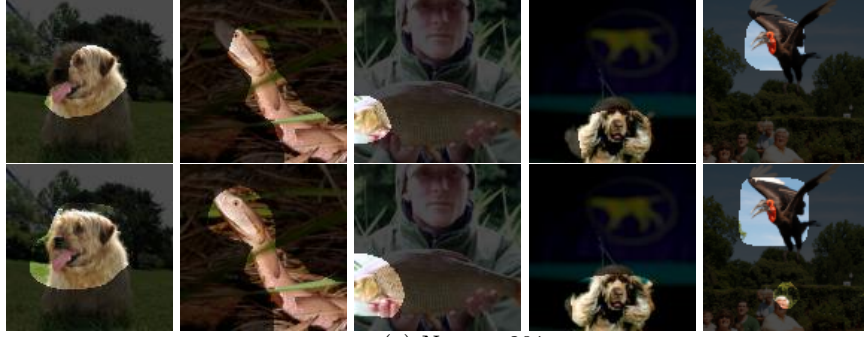


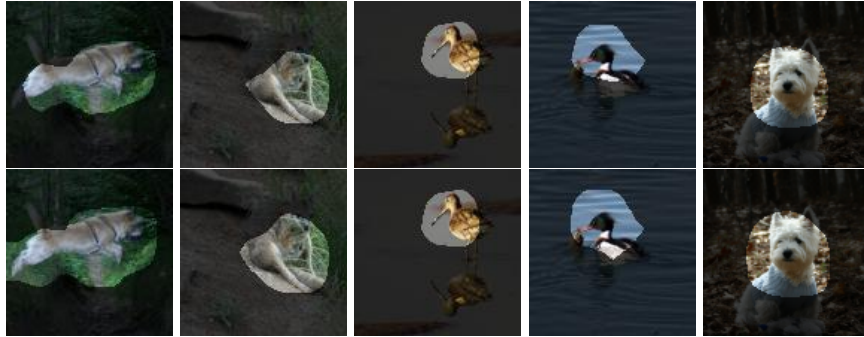
Fig. 4: Image segmentation results of sensitive neurons on benign (top line) and adversarial examples (bottom line). (a), (b) and (c) represent sensitive neuron 430, 321 and 114 in the *pool5* layer of VGG-16 Vanilla model on ImageNet, respectively. After adversarial attack, sensitive neurons tend to pay more attention to the noisy backgrounds and other meaningless regions, compared to their subtle detection regions on benign examples.



(a) Neuron 201



(b) Neuron 32



(c) Neuron 282

Fig. 5: Image segmentation results of vanilla neurons on benign (top line) and adversarial examples (bottom line). (a), (b) and (c) represent vanilla neuron 201, 32 and 282 in the *pool5* layer of VGG-16 Vanilla model on ImageNet, respectively. The Region of Interests for vanilla neurons show almost no differences between benign and adversarial examples.

neurons are quite similar. In other words, sensitive neurons make the most non-trivial contributions to model predictions in adversarial settings and uncover the strongest model weakness.

We further explore the behaviors of sensitive neurons in adversarial settings by showing what they detect during inference through visualization studies. Following the work in [47], we investigate the region of interest for different neurons (e.g., sensitive neurons and vanilla ones) on ImageNet with VGG-16 using the image segmentation based method. Due to the limited space, we only show top-3 most typical neurons of each set, i.e., the sensitive neurons with the highest sensitivity and vanilla neurons with the lowest sensitivity. For each neuron, we first find top-5 images with the highest activation in the benign sample set and then visualize image segmentation results of them and their corresponding adversarial examples generated by PGD attack. According to visualization results in Figure 4, after the adversarial attack, sensitive neurons tend to pay more attention to noisy backgrounds and other meaningless regions, compared to their subtle detection regions on benign examples. However, as shown in Figure 5, image segmentation results of vanilla neurons show almost no differences between benign and adversarial examples. With the above observation, we can double confirm the conclusion that sensitive neurons are more sensitive to adversarial noises and play critical roles to model’s final decisions in the adversarial setting. Experimental results of VGG-16 on CIFAR-10 and AlexNet on ImageNet reported in the Supplementary Material convey the same conclusion.

3.3 Sensitive Neurons Reveal Vulnerable Directions to Adversarial Weakness

We further explore characteristics of sensitive neurons at layers of different depths. PGD method is used to generate targeted adversarial examples on CIFAR-10 with VGG-16. For each class in CIFAR-10, 9000 adversarial samples are generated leading to 9000 corresponding dual pairs, which will be used to select sensitive neurons set $\Omega_l^1, \dots, \Omega_l^Y$, where l denotes the index of layer we use and Y is 10 in this case. We adopt the symbol y to stand for the target label index, i.e., $y = 1, \dots, Y$. To measure the similarity of these sets in one specific layer l , we utilize the following two metrics:

Average pair Jaccard index is used to represent the average case of the overlap between two different sets in layer l , which is defined as follow:

$$J_{avg}(\Omega_l^1, \dots, \Omega_l^Y) = \frac{1}{M} \sum_{\substack{y \neq y' \\ 1 \leq y, y' \leq Y}} J(\Omega_l^y, \Omega_l^{y'}), \quad (7)$$

where M denotes the total pair number and J is the standard Jaccard index function.

Total Jaccard index is introduced to simultaneously measure the common similarity of all sensitive neuron sets Ω_l^y in layer l . Specifically, it can be char-

acterized by the common overlap of these sets:

$$J_{total}(\Omega_l^1, \dots, \Omega_l^Y) = \frac{|\bigcap_{y=1}^Y \Omega_l^y|}{|\bigcup_{y=1}^Y \Omega_l^y|}. \quad (8)$$

As shown in Figure 2 (b), we draw a very important observation that the sensitive neurons in different target set vary a lot in the top layers, but have high similarities in the bottom layers, though they are attacked by adversarial examples with different target labels. The reason may lie in the hierarchical information processing structure of DNNs, since bottom layers focus on common low-level features, e.g., edges and textures, while top layers care more about high-level semantic features to specific classes [45]. This interesting finding indicates that different targeted adversarial examples tend to share the same flaws of bottom layers, while utilizing different fragile neurons in the top layers. Moreover, according to the results, the most sensitive neuron of the linear layer for each target set exactly corresponds to the targeted attack label. This uncovers the essence of targeted adversarial attacks that these elaborately designed noises perform the adversarial attack by increasing the logits of the target label, which is consistent with the goal of targeted attack: increasing the probability of target label. In conclusion, sensitive neurons effectively reveal vulnerable directions to adversarial weakness, which are the severe flaws leveraged by adversarial attacks. More results can be found in the Supplementary Material.

3.4 Sensitive Neurons Convey Strong Semantic Information

As we have moved so far, we prefer to move further to give more insights about the roles of sensitive neurons. Prior studies have shown the ability to use suppression and ablation skills to study individual unit functions within a model [47,48]. Thus, in this section, we try to suppress the outputs of top-10% sensitive neurons by multiplying them with a coefficient β after activation (Vanilla model is obtained when $\beta=1.0$).

As shown in Figure 3 (a), at the beginning, with the decreasing of β from 1.0, the adversarial robustness increases, while the clean example accuracy drops drastically. The model robustness nearly reaches the best when β is around 0.85. After that, when we continue to decrease the value of β , unfortunately, the model performance collapses in terms of both robustness and clean accuracy, when β reaches about 0.7. From the figure, we can conclude that: (1) there indeed exists a trade-off between robustness and accuracy [40]. (2) Sensitive neurons are responsible for both clean accuracy and robustness, indicating that they can extract strong semantic features for deep models, and will hurt model predictions a lot when suppressed.

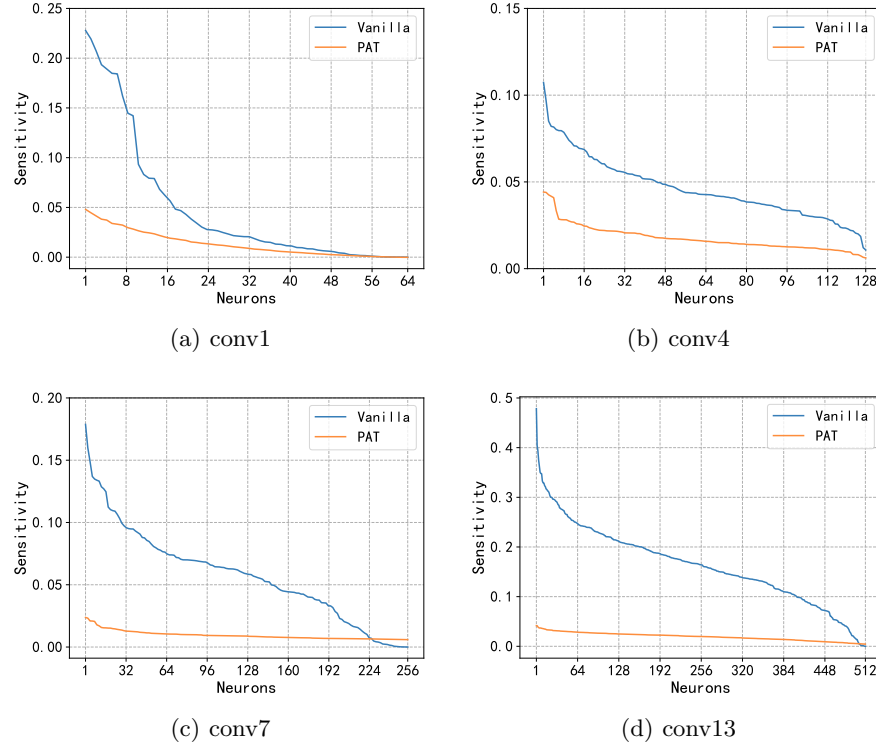


Fig. 6: Neuron sensitivity under PGD attack of all neurons on different layers (*conv1*, *conv4*, *conv7* and *conv13* from Subfigure (a) to (d)) with Vanilla and PAT trained VGG-16 on CIFAR-10. The neuron sensitivities for almost all neurons in all layers drop significantly on PAT, compared to the Vanilla model.

4 Improving Robustness with Sensitive Neurons

We have demonstrated the close connections between neuron sensitivity and adversarial robustness, as well as the basic properties of sensitive neurons in deep models. With the above observations and conclusions, it is natural to improve model robustness by stabilizing those sensitive neurons. Therefore, in this section, we first try to explore the reasons why state-of-the-art adversarial training strategies achieve strong robustness from the view of sensitive neurons. Then, we come up with a strategy called *Sensitive Neuron Stabilizing* (SNS) to alleviate the hazard brought by adversarial examples and improve model robustness by reducing the sensitivity of sensitive neurons. As the *Sensitive Neuron* are related to the used dataset and the applied adversarial attack method, we decide to use the one of the most powerful attack method PGD and the used training set to generate the adversarial examples.

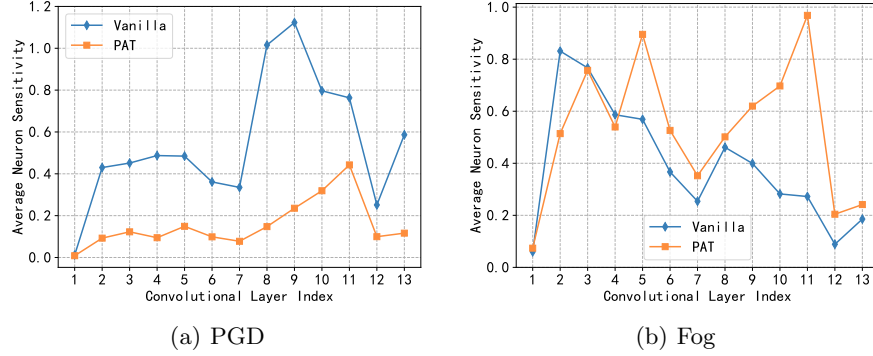


Fig. 7: Mean values of neuron sensitivities of sensitive neurons on all convolutional layers with Vanilla and PAT trained VGG-16 models on CIFAR-10. Subfigure (a) to (b) represent the situation of *PGD*, *Fog*, respectively. There exists a strong connection between neuron sensitivities and model accuracy towards noises.

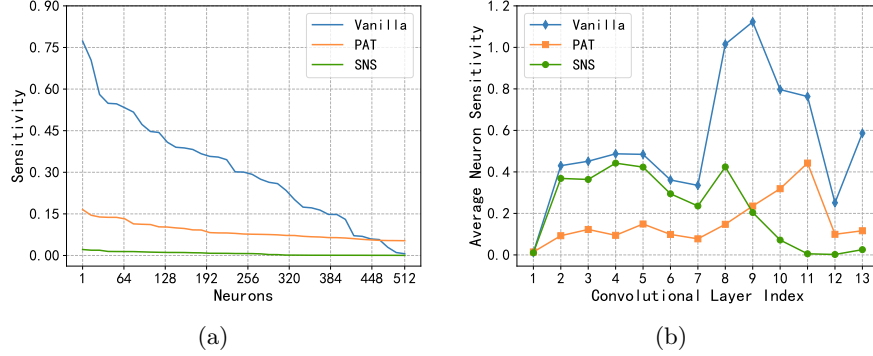


Fig. 8: Neuron sensitivity under PGD attack of sensitive neurons with Vanilla, PAT and SNS_{sen}^{adv} trained VGG-16 models on CIFAR-10. Subfigure (a) to (b) represent neuron sensitivities of all neurons on *conv10* layer and the mean values of neuron sensitivities for all convolutional layers, respectively. Our method dramatically decreases the neuron sensitivity and achieves better results than PAT.

To begin with, we use the PGD white-box attack and training set to generate sufficient dual pairs (x, x') . Next, we calculate the *Neuron Sensitivity* and obtain the *Sensitive Neuron* of each layer.

4.1 Adversarial Training Builds Robust Models by Reducing Neuron Sensitivities

With the increasing concerns of adversarial examples to model robustness, plenty of adversarial defense methods have been proposed including adversarial training, input transformation, etc. However, as discussed in [1], most of these defense

strategies just give a false sense of safety, which could be attacked easily through obfuscated gradient circumvent. Whereas, adversarial training based methods, which augment training data with adversarial examples, are relatively immune to these attacks and achieve the most robust models so far. Based on that, a number of works have been proposed to study and explain the essence of adversarial training to model robustness. Goodfellow *et al.* [11] first introduced the adversarial training strategy to defense adversarial attack by somewhat reducing the linearity for high-dimensional DNNs. Shaham *et al.* [33] tried to explain the performance of adversarial training from the view of robust optimization theory, which improves model robustness by increasing local stability.

Different from them, in this part, attempts have been made to interpret adversarial training from the perspective of neuron sensitivity. One important take-away is: *adversarial training improves model robustness by embedding representation insensitivities*.

To demonstrate this point, at the beginning, we respectively trained a Vanilla and a PGD-based adversarial training (PAT) model using VGG-16 on CIFAR-10. The white-box PGD, FGSM, Step-LL and MI-FGSM are applied as the attack method. Then, for a specific layer, we can rank its neurons according to their sensitivities. As shown in Figure 6, all neurons are extremely insensitive to adversarial examples on PAT, compared with the Vanilla model on each layer. This observation clarifies the reason why adversarial training methods are insensitive or robust to adversarial noises. Meanwhile, we witness one interesting phenomenon that the differences of the neuron sensitivity between Vanilla and PAT for the top 10% of the neurons are distinctly larger than that of others, which proves the rationality of sensitive neurons. In other words, sensitive neurons are significant indicators to represent model behaviors in the adversarial setting between benign and adversarial examples.

After neuron-wise analysis, further investigation has been made in an overall view by different layers. As shown in Figure 7 (a), under PGD attack, PAT obtains the lower sensitivity value of sensitive neurons (top 10%) with big margins compared with Vanilla model, which explains why PAT enjoys much higher adversarial robustness. Moreover, we find a very interesting phenomenon in Figure 7 (b) that in fog noise setting the neuron sensitivity values of PAT are higher than that of Vanilla model in most layers. Actually, the accuracy of Vanilla and PAT on fog noise is 33.64% and 55.64% respectively, which further confirms that the neuron sensitivity serves as a distinct indicator of model robustness.

In this point of view, we believe that, with the help of stable neurons, adversarial noises are more easily absorbed and filtered during the forward propagation process, due to the insensitive hidden representations, which in turn promises consistent model behaviors and strong robustness.

4.2 Training Adversarially Robust Models via Sensitive Neurons Stabilizing

Motivated by our observations, a straightforward idea for improving model robustness is to force the sensitive neurons of benign and adversarial ones to behave

similarly. In other words, we try to stabilize those sensitive neurons, and thus the whole model will be insensitive to adversarial examples. The *Sensitive Neurons Stabilizing* (SNS for short) can be easily accomplished by directly adding a loss term to measure the similarities of sensitive neurons behaviors when inputting the clean and adversarial examples:

$$\mathcal{L}_{sns}(x, x'; \theta) = \sum_l \sum_{F_l^m \in \Omega_l} \|F_l^m(x) - F_l^m(x')\|_1, \quad (9)$$

where \mathbf{S} denotes the indices of selected layers and Ω_l denotes *sensitive neuron* set of layer l .

Given clean examples x and adversarial examples x' , our SNS method minimizes the following loss:

$$\mathcal{L}_{cls}(x, y; \theta) + \lambda \cdot \mathcal{L}_{sns}(x, x'; \theta), \quad (10)$$

where \mathcal{L}_{cls} denotes the cross entropy loss and \mathcal{L}_{sns} represents the similarity of sensitive neurons' behaviors in some specific layers for the dual pair (x, x') . Here, λ is a hyper-parameter balancing the two loss terms.

Algorithm 1 Improve model robustness with *Sensitive Neurons Stabilizing*

Input: training set \mathbf{D} with N samples, Vanilla model $F_{Vanilla}$

Output: robust model F_{Robust}

Hyper-parameter: λ , batchsize B and epoch E

- 1: Use PGD white-box attack to generate dual pair set $\bar{\mathbf{D}} = \{(x_i, x'_i) \mid i = 1, \dots, N\}$ and select *Sensitive Neurons*.
 - 2: **for** E training epochs **do**
 - 3: **for** $\lfloor \frac{N}{B} \rfloor$ mini-batch numbers **do**
 - 4: optimize the current model by
 $\mathcal{L}_{adv}(x, x', y; \theta) + \lambda \mathcal{L}_{sns}(x, x'; \theta)$
 - 5: **end for**
 - 6: **end for**
-

As there are numerous layers in the architecture of deep models, a question emerges: *do we need to select all layers when performing SNS training?* Since different hidden layers behave variously from each other [46], it seems necessary to come up with a strategy for choosing the desired hidden layers. As discussed before that sensitive neurons that are more close to predictions reveal more adversarial weaknesses towards adversarial attacks. Meanwhile, they contain more high-level semantic information contributing to the model's final decisions. Thus, we conduct experiments of training models with top- k hidden layers to figure out the choices for layer selection. Namely, parameters of the bottom several layers are locked during finetuning. As illustrated in Figure 3 (b), using layers from *conv8* to *conv13* reaches the most adversarially robust model. Thus, the rest of the paper follows this guidance.

Firstly, we try to test model robustness by using our proposed SNS on CIFAR-10 with VGG-16. We adopt Step-LL, MI-FGSM, FGSM and PGD as

Table 1: Experiments result of adversarial robustness test on CIFAR-10 with VGG-16. Our strategy outperforms all comparison methods towards adversarial examples generated by different attack methods.

MODEL	CLEAN	TARGETED ATTACK		UNTARGETED ATTACK	
		STEP-LL	MI-FGSM	PGD	FGSM
VANILLA	89.19%	7.99%	3.10%	0.00%	4.88%
NAT	88.59%	39.57%	21.12%	1.05%	26.72%
EAT	87.84%	41.88%	35.72%	16.24%	27.87%
PAT	85.16%	74.94%	76.36%	46.04%	46.96%
ALP	81.41%	71.06%	76.90%	44.76%	46.80%
SNS_{sen}^{cls}	91.29%	48.89%	36.52%	16.95%	42.68%
SNS_{all}^{cls}	90.72%	47.08%	32.33%	9.27%	35.27%
SNS_{sen}^{adv}	87.24%	77.08%	79.53%	48.47%	49.16%

Table 2: Experiments result of adversarial robustness test on ImageNet with AlexNet. Our strategy outperforms all comparison methods towards adversarial examples generated by different attack methods.

MODEL	CLEAN	TARGETED ATTACK		UNTARGETED ATTACK	
		STEP-LL	MI-FGSM	PGD	FGSM
VANILLA	57.70%	34.10%	33.75%	10.50%	13.85%
NAT	55.46%	34.23%	33.79%	9.07%	12.63%
EAT	56.13%	38.77%	38.54%	13.01%	15.77%
PAT	55.10%	49.28%	50.89%	26.44%	27.83%
SNS_{sen}^{cls}	59.10%	37.01%	37.28%	13.15%	16.47%
SNS_{sen}^{adv}	56.35%	51.14%	53.05%	28.53%	30.72%

the adversarial attack methods in this section. We first train model with the loss in Equation 10 using top-10% sensitive neurons, and from Table 1 we can see that our model (SNS_{sen}^{cls}) outperforms NAT and EAT model for white-box adversarial defense in all cases, which indicates the effectiveness of improving model robustness by constraining sensitive neurons.

Secondly, to examine the superiority of using sensitive neurons compared with all neurons for improving model robustness, we conduct a comparative experiment. As shown in Table 1 (SNS_{all}^{cls}), the model’s adversarial robustness decreases to some extent, which means that sensitive neurons are more critical for adversarial robustness, while constraining all neurons may somewhat lead to the drop of adversarial robustness. The reason might be that using vanilla neurons will introduce meaningless gradients, which is harmful for improving the model’s robustness.

Finally, in order to further improve model robustness, we introduce another version of sensitive neurons stabilizing loss, which adopts adversarial training

loss instead of normal cross entropy loss:

$$\mathcal{L}_{adv}(x, x', y; \theta) + \lambda \mathcal{L}_{sns}(x, x'; \theta), \quad (11)$$

where \mathcal{L}_{adv} denotes the adversarial training loss. The whole training process is demonstrated in Algorithm 1.

According to [18], ALP is implemented on the basis of PGD-based adversarial training. Therefore, for fair comparisons, we use the adversarial version of SNS here as SNS_{sen}^{adv} . According to the result (SNS_{sen}^{adv}) in Table 1, our method outperforms all other comparison methods including PAT and ALP, indicating that SNS builds strong models towards adversarial examples. However, we notice that ALP and PAT decrease the model performance on clean examples drastically. Meanwhile, ALP also shows weak adversarial defense ability in most cases compared with PAT. These observations prove the importance of using sensitive neurons for improving model robustness compared with logits (ALP). Furthermore, stabilizing sensitive neurons also serves as a regularization term when used with adversarial training loss to alleviate clean example accuracy drops, since most adversarial training strategies build models with relatively low clean example accuracy. The corresponding experimental results on ImageNet with AlexNet are shown in Table 2.

Since our model (SNS_{sen}^{adv}) reaches the best performance of adversarial robustness, we make further analyses on how the neuron sensitivity changes after SNS training. Figure 8 (a) shows the neuron sensitivity of all neurons in *conv10* layer after SNS training. It is obvious that our method dramatically suppresses the neuron sensitivity and achieves better results than PAT, which demonstrates that SNS loss term significantly contributes to better adversarial robustness. Further, our method requires much fewer epochs compared to PAT, leading to less time consumption. As illustrated in Figure 8 (b), interestingly, the sensitivities of neurons on layer *conv8* to *conv13* have a significant change, which exactly match layers we use in SNS to train the model. Meanwhile, the neuron sensitivities in bottom layers stay high since they were fixed and only *conv8* to *conv13* were finetuned during training.

5 Conclusion

In this paper, we attempt to interpret and improve adversarial robustness for deep models from a new perspective of neuron sensitivity which is measured by neuron behavior variation intensity against benign and adversarial examples. By thorough analyses, we first draw the close relationship between adversarial robustness and neuron sensitivities, as sensitive neurons make the most non-trivial contribution to model predictions in the adversarial setting. Based on that conclusion, we further propose to improve model robustness against adversarial examples by sensitive neurons stabilizing which constrains the behaviors of sensitive neurons between benign and adversarial examples. Moreover, state-of-the-art adversarial training strategies also achieve strong robustness by reducing neuron sensitivities which in turn confirms the importance of sensitive neurons

to model robustness in the adversarial setting. Extensive experiments on various datasets demonstrate that our algorithm effectively achieves excellent results.

References

1. Athalye, A., Carlini, N., Wagner, D.: Obfuscated gradients give a false sense of security: Circumventing defenses to adversarial examples. In: ICML (2018)
2. Bai, Y., Feng, Y., Wang, Y., Dai, T., Xia, S.T., Jiang, Y.: Hilbert-based generative defense for adversarial examples. In: ICCV (2019)
3. Bau, D., Zhou, B., Khosla, A., Oliva, A., Torralba, A.: Network dissection: Quantifying interpretability of deep visual representations. In: CVPR (2017)
4. Carlini, N., Wagner, D.: Towards evaluating the robustness of neural networks. In: S&P (2017)
5. Chen, D., Manning, C.: A fast and accurate dependency parser using neural networks. In: EMNLP (2014)
6. Dong, Y., Liao, F., Pang, T., Su, H., Zhu, J., Hu, X., Li, J.: Boosting adversarial attacks with momentum. In: CVPR (2018)
7. Dong, Y., Su, H., Zhu, J., Bao, F.: Towards interpretable deep neural networks by leveraging adversarial examples. CoRR **abs/1708.05493** (2017), <http://arxiv.org/abs/1708.05493>
8. Dziugaite, G.K., Ghahramani, Z., Roy, D.M.: A study of the effect of JPG compression on adversarial images. CoRR **abs/1608.00853** (2016), <http://arxiv.org/abs/1608.00853>
9. Engstrom, L., Ilyas, A., Santurkar, S., Tsipras, D., Tran, B., Madry, A.: Learning perceptually-aligned representations via adversarial robustness. CoRR **abs/1906.00945** (2019), <http://arxiv.org/abs/1906.00945>
10. Gao, J., Wang, B., Lin, Z., Xu, W., Qi, Y.: Deepcloak: Masking deep neural network models for robustness against adversarial samples. In: ICLR Workshop (2017), https://openreview.net/forum?id=r1X_kR4Yl
11. Goodfellow, I.J., Shlens, J., Szegedy, C.: Explaining and harnessing adversarial examples. In: ICLR (2015), <http://arxiv.org/abs/1412.6572>
12. Guo, C., Gardner, J., You, Y., Wilson, A.G., Weinberger, K.: Simple black-box adversarial attacks. In: ICML (2019)
13. Guo, C., Rana, M., Cissé, M., van der Maaten, L.: Countering adversarial images using input transformations. In: ICLR (2018), <https://openreview.net/forum?id=SyJ7C1WCb>
14. He, K., Zhang, X., Ren, S., Sun, J.: Deep residual learning for image recognition. In: CVPR (2016). <https://doi.org/10.1109/CVPR.2016.90>, <https://doi.org/10.1109/CVPR.2016.90>
15. Ilyas, A., Santurkar, S., Tsipras, D., Engstrom, L., Tran, B., Madry, A.: Adversarial examples are not bugs, they are features. CoRR **abs/1905.02175** (2019), <http://arxiv.org/abs/1905.02175>
16. Inkawhich, N., Wen, W., Li, H.H., Chen, Y.: Feature space perturbations yield more transferable adversarial examples. In: CVPR (2019), http://openaccess.thecvf.com/content_CVPR_2019/html/Inkawhich_Feature_Space_Perturbations_Yield_More_Transferable_Adversarial_Examples_CVPR_2019_paper.html
17. Jang, Y., Zhao, T., Hong, S., Lee, H.: Adversarial defense via learning to generate diverse attacks. In: ICCV (2019)

18. Kannan, H., Kurakin, A., Goodfellow, I.J.: Adversarial logit pairing. CoRR **abs/1803.06373** (2018), <http://arxiv.org/abs/1803.06373>
19. Krizhevsky, A., Hinton, G.: Learning multiple layers of features from tiny images. Tech. rep., Citeseer (2009)
20. Krizhevsky, A., Sutskever, I., Hinton, G.E.: Imagenet classification with deep convolutional neural networks. In: NeurIPS (2012), <http://papers.nips.cc/paper/4824-imagenet-classification-with-deep-convolutional-neural-networks>
21. Kurakin, A., Goodfellow, I.J., Bengio, S.: Adversarial examples in the physical world. In: ICLR (2017), <https://openreview.net/forum?id=HJGU3Rodl>
22. Kurakin, A., Goodfellow, I.J., Bengio, S.: Adversarial machine learning at scale. In: ICLR (2017), <https://openreview.net/forum?id=BJm4T4KgX>
23. Liao, F., Liang, M., Dong, Y., Pang, T., Hu, X., Zhu, J.: Defense against adversarial attacks using high-level representation guided denoiser. In: CVPR (2018)
24. Liu, A., Liu, X., Fan, J., Ma, Y., Zhang, A., Xie, H., Tao, D.: Perceptual-sensitive gan for generating adversarial patches. In: AAAI (2019)
25. Lu, J., Issaranoon, T., Forsyth, D.A.: Safetynet: Detecting and rejecting adversarial examples robustly. In: ICCV (2017). <https://doi.org/10.1109/ICCV.2017.56>, <https://doi.org/10.1109/ICCV.2017.56>
26. Madry, A., Makelov, A., Schmidt, L., Tsipras, D., Vladu, A.: Towards deep learning models resistant to adversarial attacks. In: ICLR (2018), <https://openreview.net/forum?id=rJzIBfZAb>
27. Metzen, J.H., Genewein, T., Fischer, V., Bischoff, B.: On detecting adversarial perturbations. In: ICLR (2017), <https://openreview.net/forum?id=SJzCSf9xg>
28. Mohamed, A., Dahl, G.E., Hinton, G.E.: Acoustic modeling using deep belief networks. IEEE Trans. Audio, Speech & Language Processing (2012). <https://doi.org/10.1109/TASL.2011.2109382>, <https://doi.org/10.1109/TASL.2011.2109382>
29. Papernot, N., McDaniel, P.D., Wu, X., Jha, S., Swami, A.: Distillation as a defense to adversarial perturbations against deep neural networks. In: S&P (2016). <https://doi.org/10.1109/SP.2016.41>, <https://doi.org/10.1109/SP.2016.41>
30. Ren, S., He, K., Girshick, R.B., Sun, J.: Faster R-CNN: towards real-time object detection with region proposal networks. In: NeurIPS (2015), <http://papers.nips.cc/paper/5638-faster-r-cnn-towards-real-time-object-detection-with-region-proposal-networks>
31. Roth, K., Kilcher, Y., Hofmann, T.: The odds are odd: A statistical test for detecting adversarial examples. In: ICML (2019)
32. Russakovsky, O., Deng, J., Su, H., Krause, J., Satheesh, S., Ma, S., Huang, Z., Karpathy, A., Khosla, A., Bernstein, M.S., Berg, A.C., Li, F.: Imagenet large scale visual recognition challenge. IJCV (2015). <https://doi.org/10.1007/s11263-015-0816-y>, <https://doi.org/10.1007/s11263-015-0816-y>
33. Shaham, U., Yamada, Y., Negahban, S.: Understanding adversarial training: Increasing local stability of supervised models through robust optimization. Neurocomputing (2018)
34. Simonyan, K., Zisserman, A.: Very deep convolutional networks for large-scale image recognition. In: ICLR (2015), <http://arxiv.org/abs/1409.1556>
35. Song, D., Eykholt, K., Evtimov, I., Fernandes, E., Li, B., Rahmati, A., Tramèr, F., Prakash, A., Kohno, T.: Physical adversarial examples for object detectors. In: WOOT (2018), <https://www.usenix.org/conference/woot18/presentation/eykholt>

36. Su, J., Vargas, D.V., Sakurai, K.: One pixel attack for fooling deep neural networks. *IEEE Trans. Evolutionary Computation* (2019). <https://doi.org/10.1109/TEVC.2019.2890858>, <https://doi.org/10.1109/TEVC.2019.2890858>
37. Sutskever, I., Vinyals, O., Le, Q.V.: Sequence to sequence learning with neural networks. In: *NeurIPS*. pp. 3104–3112 (2014), <http://papers.nips.cc/paper/5346-sequence-to-sequence-learning-with-neural-networks>
38. Szegedy, C., Zaremba, W., Sutskever, I., Bruna, J., Erhan, D., Goodfellow, I.J., Fergus, R.: Intriguing properties of neural networks. In: *ICLR* (2014), <http://arxiv.org/abs/1312.6199>
39. Tramèr, F., Kurakin, A., Papernot, N., Goodfellow, I.J., Boneh, D., McDaniel, P.D.: Ensemble adversarial training: Attacks and defenses. In: *ICLR* (2018), <https://openreview.net/forum?id=rkZvSe-RZ>
40. Tsipras, D., Santurkar, S., Engstrom, L., Turner, A., Madry, A.: Robustness may be at odds with accuracy. In: *ICLR* (2019), <https://openreview.net/forum?id=SyxAb30cY7>
41. Xie, C., Wang, J., Zhang, Z., Ren, Z., Yuille, A.L.: Mitigating adversarial effects through randomization. In: *ICLR* (2018), <https://openreview.net/forum?id=Sk9yuql0Z>
42. Xu, H., Mannor, S.: Robustness and generalization. *Machine learning* (2012)
43. Xu, K., Liu, S., Zhang, G., Sun, M., Zhao, P., Fan, Q., Gan, C., Lin, X.: Interpreting adversarial examples by activation promotion and suppression. *CoRR* **abs/1904.02057** (2019), <http://arxiv.org/abs/1904.02057>
44. Xu, W., Evans, D., Qi, Y.: Feature squeezing: Detecting adversarial examples in deep neural networks. In: *NDSS* (2018), http://wp.internetsociety.org/ndss/wp-content/uploads/sites/25/2018/02/ndss2018_03A-4_Xu_paper.pdf
45. Zeiler, M.D., Fergus, R.: Visualizing and understanding convolutional networks. In: *ECCV* (2014). https://doi.org/10.1007/978-3-319-10590-1_53, https://doi.org/10.1007/978-3-319-10590-1_53
46. Zhang, C., Bengio, S., Singer, Y.: Are all layers created equal? *CoRR* **abs/1902.01996** (2019), <http://arxiv.org/abs/1902.01996>
47. Zhou, B., Khosla, A., Lapedriza, À., Oliva, A., Torralba, A.: Object detectors emerge in deep scene cnns. In: *ICLR* (2015), <http://arxiv.org/abs/1412.6856>
48. Zhou, B., Lapedriza, À., Xiao, J., Torralba, A., Oliva, A.: Learning deep features for scene recognition using places database. In: *NeurIPS* (2014), <http://papers.nips.cc/paper/5349-learning-deep-features-for-scene-recognition-using-places-database>

A Empirical Analysis Details

In this section, we will give some details of our methods and measurements used in the empirical analysis section.

A.1 Weighted Voting Method

In order to select the Important Neurons set I^y to one adversarial example set \mathbf{D}' for a specific target class y , we apply a weighted voting method ρ . Specifically, an Important Neurons $II^y(x_i)$ contains k_1 neurons which are ranked in descending order by sensitivity. To emphasize their different importances, we give them different votes from k_1 to 1. After the voting process, votes for each neuron will be counted and the top- k_2 of them will be selected. In our experiment, we choose $k_1 = k_2 = 20$.

B More Experiment Results

In this section, we will give more experiment results.

B.1 Sensitive Neurons Reveal Vulnerable Directions to Adversarial Weakness

In the empirical analysis part, we have demonstrated the finding that sensitive neurons in different target set vary a lot in the top layers, but have high similarities in the bottom layers using VGG-16 on CIFAR-10. To further confirm it, we adopt experiment on ImageNet with AlexNet. As there are excessive classes in ImageNet, we randomly select 10 of them and apply PGD targeted attack to these target class y to generate adversarial example dataset \mathbf{D}' respectively and then obtain the sensitive neuron sets \mathcal{O}_l^y of each classes, where $l \in \{1, \dots, L\}$. *Total Jaccard index* and *average pair Jaccard index* of sensitive neuron set are computed and the results are shown in Figure 9 which double confirms the conclusion.

Moreover, we list the detailed results of sensitive neurons on 10 different targeted adversarial example sets by layers within VGG-16 on CIFAR-10. Table 3 and Table 4 list the result of several specific layers: *conv1*, *conv4*, *conv7*, *conv11*, *conv13* and *fc*. All the results are ranked in descending order by sensitivity.

B.2 Adversarial Training Improves Model Robustness by Reducing Neuron Sensitivities

In this section, we demonstrate more results about the contributions of sensitive neurons to adversarial training strategies. As shown in Figure 10, 11, the mean sensitivity values of sensitive neurons on CIFAR-10 with VGG-16 and ImageNet with AlexNet using PAT are lower than that of Vanilla model. Then, the result of ResNet-18 on CIFAR-10 is shown in Figure 12. After that, we also show the

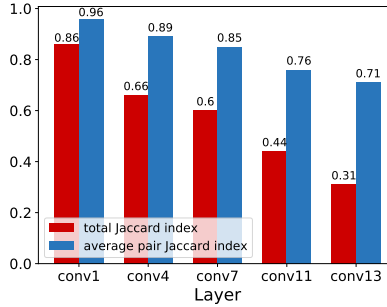


Fig. 9: Neuron similarity of PGD attack for 10 different target labels using AlexNet on ImageNet. Specifically, the total Jaccard index and average pair Jaccard index of sensitive neuron sets $\Omega_l^1, \dots, \Omega_l^{10}$. Classes are randomly selected including: *altar*, *obelisk*, *triumphal-arch*, *scorpion*, *nail*, *kimono*, *syringe*, *cliff-dwelling*, *koala* and *confectionery*.

sensitivities of all neurons on different layers of AlexNet on ImageNet in Figure 13. Above results confirm the evidence that adversarial training improves model robustness by embedding neuron insensitivity.

B.3 Sensitive Neurons contribute Most to Adversarial Misclassification

In this section, we further demonstrate the result of visualizing receptive fields of sensitive neurons and vanilla ones in two more models with same process mentioned before. The comparison of visualization result of sensitive neurons and vanilla ones on CIFAR-10 with VGG-16 is shown in Figure 14 and 15, respectively. Meanwhile, Figure 16 and 17 demonstrate the result on ImageNet with AlexNet. From these visualization results, same conclusions can be drawn as stated before that sensitive neurons contribute most to adversarial misclassification.

C Implementation Details

C.1 Adversarial Defensive Methods

In this section, the implementation details of SNS and other defensive methods are given.

SNS. PGD attack is used for generating adversarial example set from training set, based on which sensitive neurons are selected. Then we train models with different hyper-parameters on different datasets. On CIFAR-10 with VGG-16, we use the sensitive neurons from *conv8* to *conv13* with $\lambda = 5.0$ in the training set. On ImageNet with AlexNet, we use the sensitive neurons from *conv3* to *conv5* with $\lambda = 6.0$ in the training set.

NAT. Step-LL attack on current training model is used for adversarial examples generating with ϵ obtained by absolute value of normal distribution $N(0, 8)$

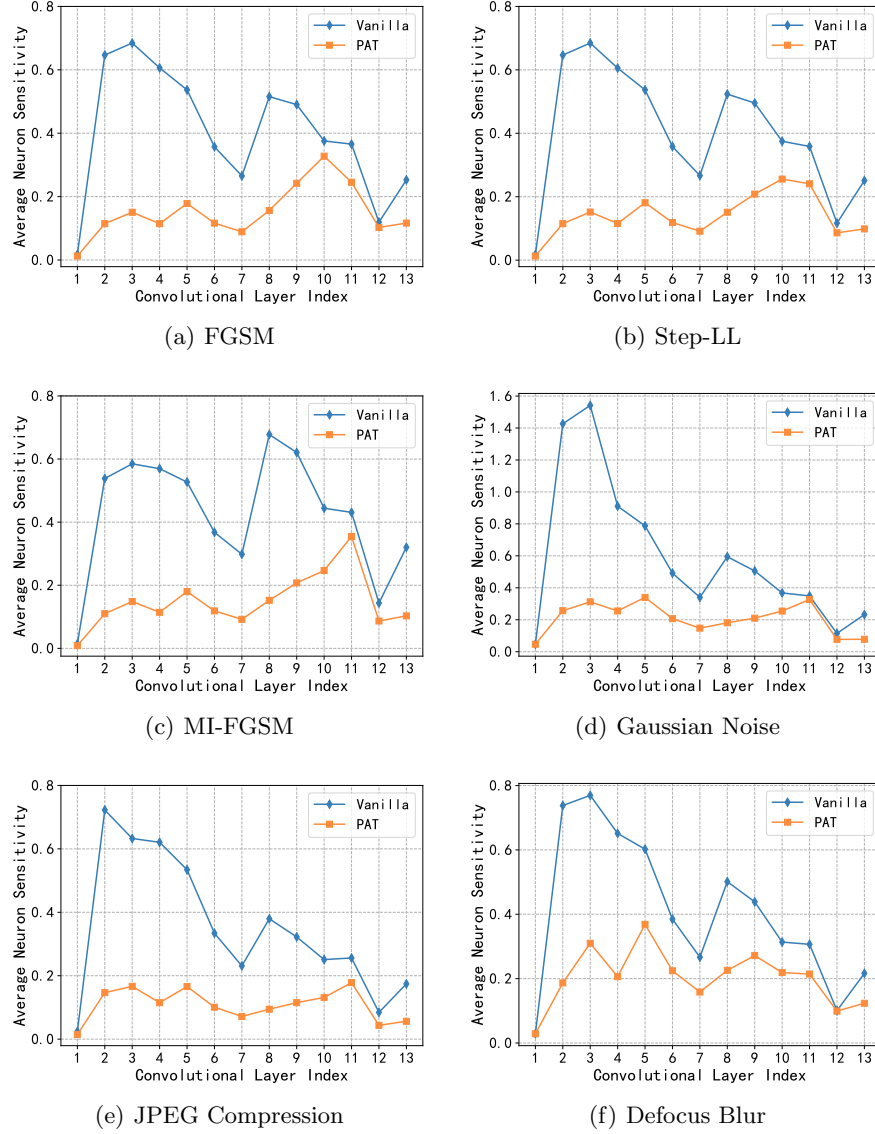


Fig. 10: Mean values of neuron sensitivity on sensitive neurons of all convolutional layers with Vanilla and PAT using VGG-16 on CIFAR-10. Subfigure (a) to (f) represent the situation of *FGSM*, *Step-LL*, *MI-FGSM*, *Gaussian Noise*, *JPEG Compression*, *Defocus Blur*, respectively.

and truncated to $[0,16]$. Meanwhile, the coefficient ratio adopted for clean and adversarial examples during the training phase are 1 to 1.

EAT. Experiment settings for EAT are the same for NAT except for the target models for adversarial example generating. On CIFAR-10, the target models

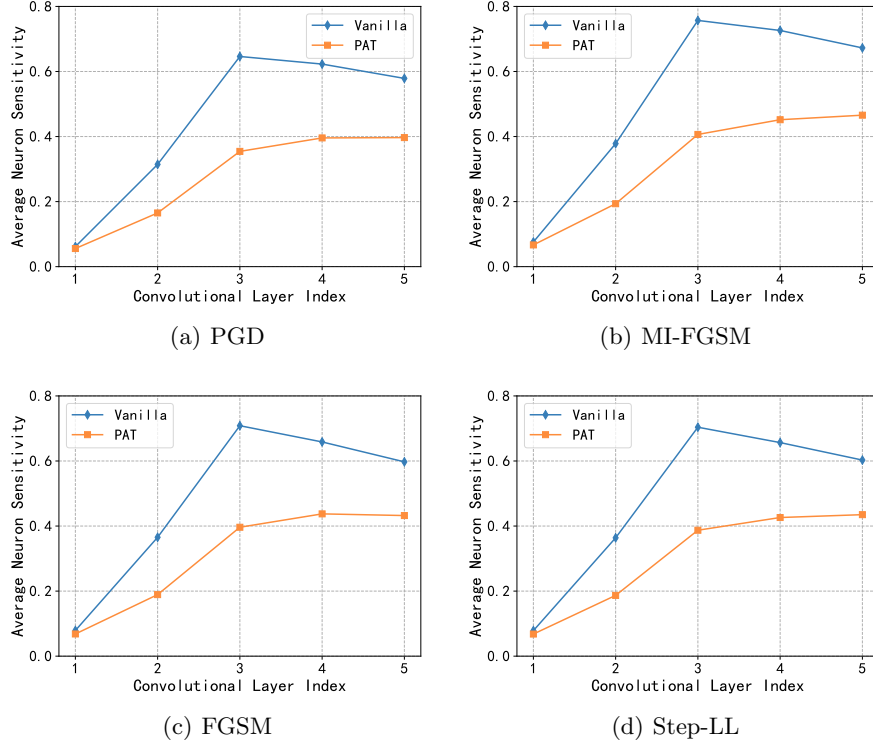
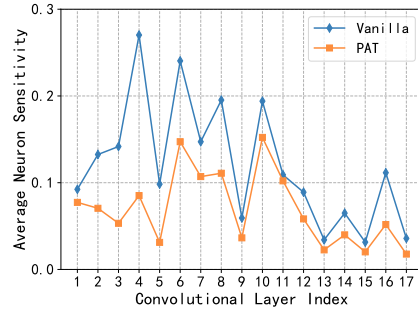


Fig. 11: Mean values of neuron sensitivity on sensitive neurons of all convolutional layers with Vanilla and PAT using AlexNet on ImageNet. Subfigure (a) to (d) represent the situation of *PGD*, *MI-FGSM*, *FGSM*, *Step-LL*, respectively.

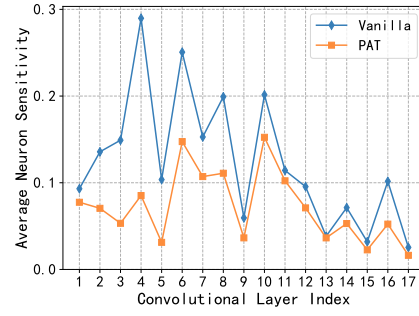
are Inception-v2, ResNet-18 and the current training model. As for ImageNet, the target models are AlexNet, ResNet-18 and the current training model.

PAT. PGD attack on current training model is used for adversarial examples generating with $\epsilon = 8, k = 10, \alpha = 0.8$. The clean and adversarial examples are mixed in the ratio of 1 to 1 during the training phase.

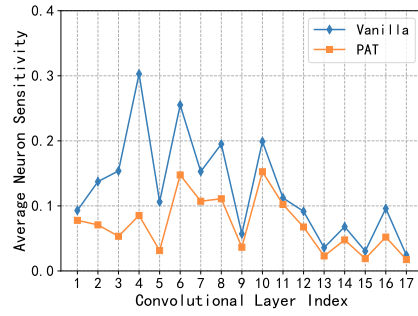
ALP. The loss terms of ALP consist of two main parts: adversarial training loss whose setting is consistent with PAT and logit pairing term which is implemented with L_2 loss. The ratio of these two terms during training phase are 2 to 1, namely the coefficient λ of logit pairing term is 0.5.



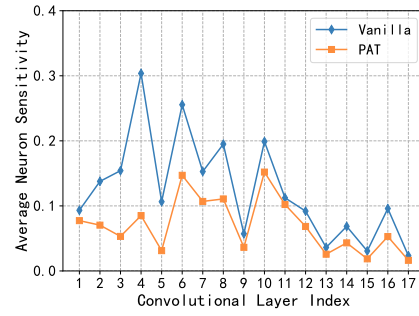
(a) PGD



(b) MI-FGSM



(c) FGSM



(d) Step-LL

Fig. 12: Mean values of neuron sensitivity on sensitive neurons of all convolutional layers with Vanilla and PAT using ResNet-18 on CIFAR-10. Subfigure (a) to (d) represent the situation of *PGD*, *MI-FGSM*, *FGSM*, *Step-LL*, respectively.

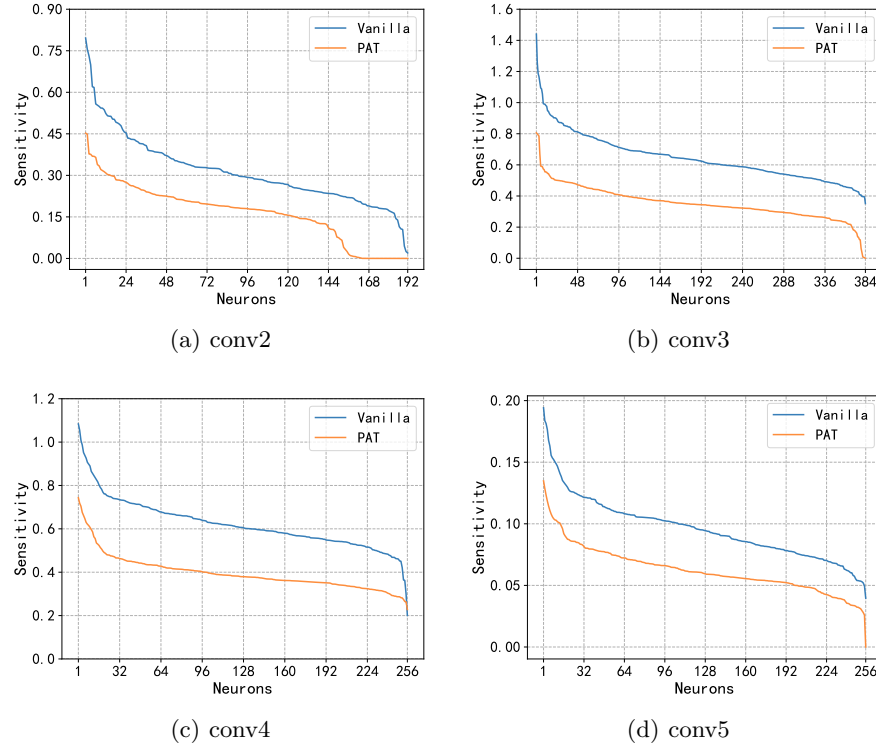
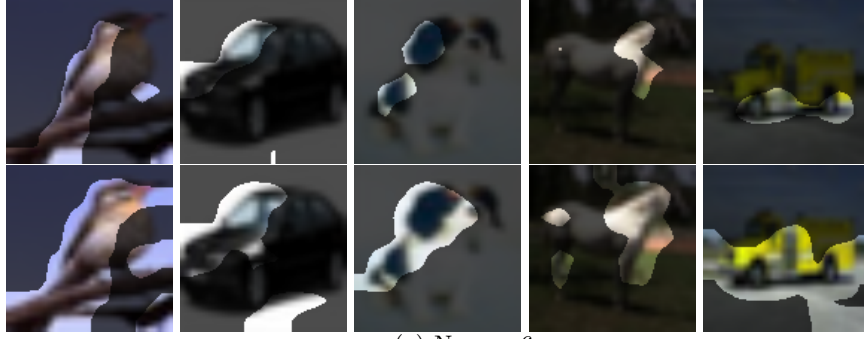
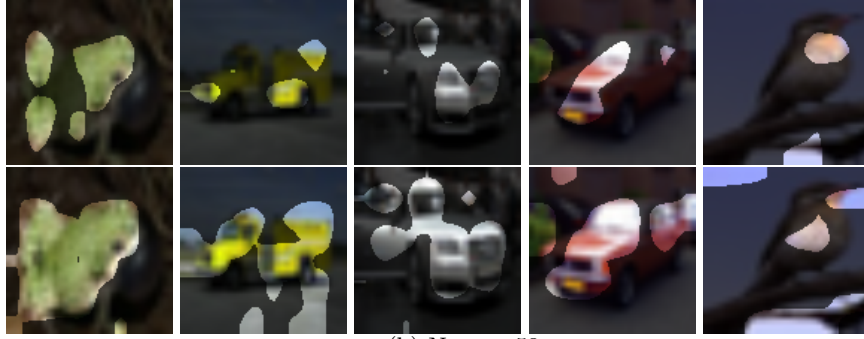


Fig. 13: Neuron sensitivity of all neurons on different layers (*conv2*, *conv3*, *conv4* and *conv5* from subfigure (a) to (d)) with Vanilla and PAT using AlexNet on ImageNet .



(a) Neuron 6



(b) Neuron 53



(c) Neuron 74

Fig. 14: Image segmentation results of sensitive neurons on benign (top line) and adversarial examples (bottom line). (a), (b) and (c) represent sensitive neuron 6, 53 and 74 in the *pool2* layer of VGG-16 Vanilla model on CIFAR-10, respectively.

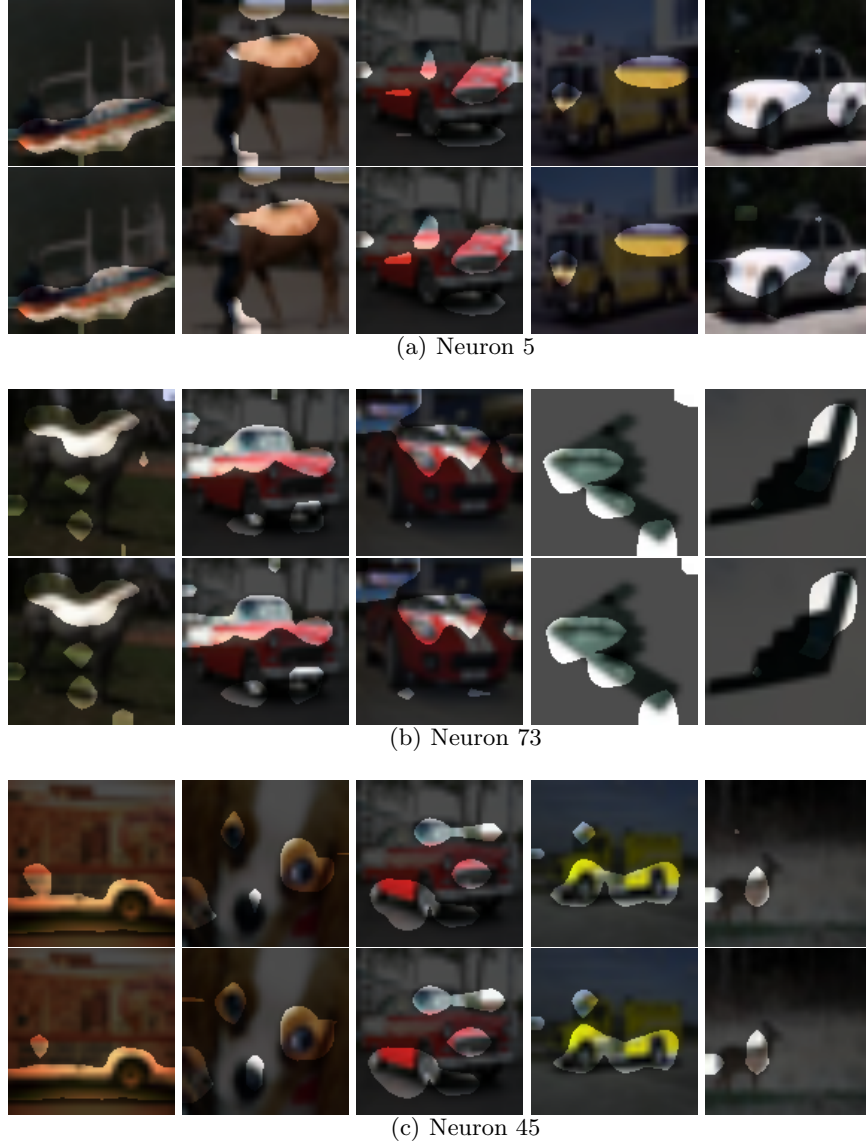
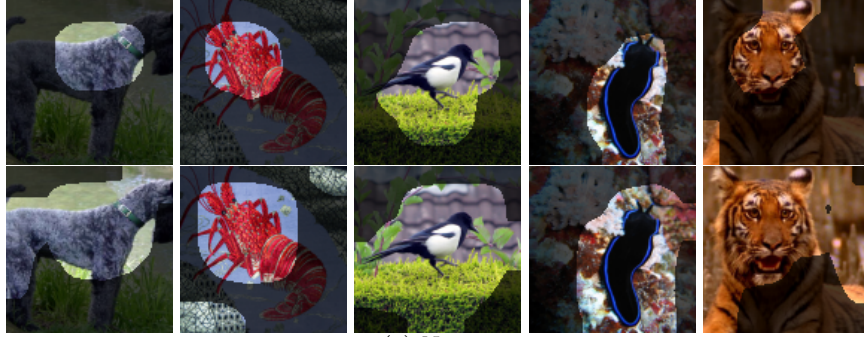


Fig. 15: Image segmentation results of vanilla neurons on benign (top line) and adversarial examples (bottom line). (a), (b) and (c) represent vanilla neuron 5, 73 and 45 in the *pool2* layer of VGG-16 Vanilla model on CIFAR-10, respectively.



(a) Neuron 112



(b) Neuron 89



(c) Neuron 136

Fig. 16: Image segmentation results of sensitive neurons on benign (top line) and adversarial examples (bottom line). (a), (b) and (c) represent sensitive neuron 112, 89 and 136 in the *pool3* layer of AlexNet Vanilla model on ImageNet, respectively.



(a) Neuron 116



(b) Neuron 32



(c) Neuron 207

Fig. 17: Image segmentation results of vanilla neurons on benign (top line) and adversarial examples (bottom line). (a), (b) and (c) represent vanilla neuron 116, 32 and 207 in the *pool3* layer of AlexNet Vanilla model on ImageNet, respectively.

Table 3: Sensitive neurons on 10 targeted adversarial example sets in *conv1*, *conv4*, *conv7* and *conv11* layer of VGG-16 on CIFAR-10.

Target Label	conv1	conv4	conv7	conv11
0	52, 10, 14, 55, 25, 15	18, 6, 111, 103, 125, 79, 58, 68, 74, 16, 1, 32	0, 72, 128, 107, 176, 10, 114, 149, 76, 105, 93, 135, 134, 9, 217, 57, 161, 19, 131, 143, 59, 148, 192, 27, 78	504, 124, 184, 428, 364, 312, 202, 264, 133, 138, 272, 257, 342, 232, 66, 119, 381, 359, 161, 224, 127, 165, 308, 336, 25, 469, 293, 349, 356, 7, 319, 418, 234, 146, 340, 211, 32, 317, 63, 305, 204, 299, 240, 360, 1, 487, 249, 92, 407, 358
1	10, 52, 14, 55, 25, 15	18, 6, 103, 111, 125, 79, 8, 74, 58, 68, 1, 9	0, 9, 128, 57, 149, 118, 72, 217, 114, 134, 7, 10, 43, 107, 143, 105, 161, 176, 76, 135, 131, 169, 93, 19, 148	184, 232, 66, 264, 428, 202, 312, 257, 342, 138, 364, 272, 133, 504, 161, 119, 381, 359, 124, 127, 165, 308, 224, 336, 25, 469, 293, 349, 356, 7, 319, 418, 146, 234, 340, 211, 32, 317, 63, 305, 204, 299, 240, 360, 1, 487, 249, 92, 407, 330
2	10, 52, 14, 55, 25, 15	18, 6, 125, 111, 103, 79, 58, 1, 74, 8, 82, 16	0, 143, 149, 128, 195, 161, 72, 134, 217, 114, 105, 78, 9, 16, 176, 93, 10, 19, 135, 118, 107, 60, 76, 131, 69	264, 184, 272, 428, 202, 312, 127, 66, 133, 138, 504, 257, 364, 342, 232, 124, 359, 161, 381, 119, 308, 336, 165, 25, 224, 469, 293, 349, 356, 7, 319, 418, 234, 340, 146, 211, 32, 63, 317, 305, 204, 299, 240, 360, 1, 487, 249, 92, 407, 368
3	10, 52, 14, 55, 25, 15	18, 6, 111, 125, 103, 79, 74, 8, 58, 1, 68, 16	0, 170, 217, 214, 128, 206, 2, 72, 233, 149, 53, 114, 41, 134, 27, 10, 135, 105, 107, 9, 76, 143, 28, 176, 249	184, 312, 428, 202, 264, 272, 232, 364, 381, 359, 138, 257, 133, 66, 504, 342, 124, 127, 119, 161, 165, 336, 308, 224, 25, 469, 293, 349, 356, 7, 319, 418, 234, 340, 146, 211, 32, 317, 63, 305, 204, 299, 240, 360, 1, 487, 249, 92, 407, 170
4	10, 52, 14, 55, 25, 15	18, 6, 125, 111, 103, 79, 58, 8, 74, 16, 1, 49	0, 19, 149, 176, 154, 43, 223, 72, 214, 128, 93, 105, 148, 57, 217, 114, 143, 10, 24, 135, 192, 59, 9, 107, 161	133, 428, 342, 202, 184, 364, 264, 504, 312, 124, 66, 272, 138, 257, 119, 359, 381, 232, 161, 224, 127, 25, 308, 165, 336, 469, 293, 349, 356, 7, 319, 418, 234, 211, 146, 340, 32, 317, 63, 305, 204, 299, 240, 360, 1, 487, 249, 92, 407, 166, 508
5	52, 10, 14, 55, 25, 15	18, 6, 111, 125, 103, 79, 58, 8, 74, 1, 16, 49	0, 217, 107, 247, 19, 76, 128, 135, 111, 79, 72, 149, 114, 143, 57, 10, 9, 134, 161, 43, 78, 175, 93, 105, 164	184, 272, 202, 312, 359, 364, 428, 264, 124, 138, 504, 119, 161, 232, 257, 381, 66, 342, 133, 127, 224, 165, 308, 25, 336, 469, 293, 349, 356, 7, 319, 418, 234, 146, 340, 211, 32, 317, 63, 305, 204, 299, 240, 360, 1, 487, 249, 92, 407, 209
6	52, 10, 14, 55, 25, 15	18, 6, 125, 111, 103, 79, 58, 1, 68, 74, 82, 16	114, 0, 131, 128, 169, 149, 10, 217, 148, 72, 134, 9, 80, 143, 30, 135, 105, 107, 176, 161, 76, 233, 57, 214, 230	138, 133, 161, 428, 364, 264, 184, 257, 202, 272, 312, 66, 504, 232, 359, 342, 127, 381, 119, 124, 308, 165, 224, 336, 25, 469, 293, 349, 356, 7, 319, 418, 234, 211, 340, 146, 32, 317, 63, 305, 204, 299, 240, 360, 1, 487, 249, 92, 407, 508
7	52, 10, 14, 55, 15, 25	18, 6, 111, 103, 125, 74, 79, 58, 8, 1, 68, 9	0, 10, 149, 114, 72, 22, 43, 107, 165, 78, 76, 25, 128, 217, 206, 168, 135, 110, 161, 105, 143, 9, 134, 176, 192	342, 119, 428, 184, 312, 264, 202, 364, 66, 133, 138, 257, 381, 165, 272, 359, 504, 232, 161, 124, 127, 308, 224, 25, 336, 469, 293, 349, 356, 7, 319, 418, 234, 146, 340, 211, 32, 317, 63, 305, 204, 299, 240, 360, 1, 487, 249, 92, 407, 483
8	52, 10, 14, 55, 25, 15	18, 6, 111, 103, 79, 125, 58, 16, 74, 8, 9, 1	134, 148, 0, 131, 128, 149, 10, 72, 73, 105, 57, 9, 143, 135, 107, 93, 217, 34, 176, 76, 114, 19, 161, 59, 80	257, 184, 428, 202, 264, 312, 138, 133, 232, 364, 504, 272, 119, 342, 124, 66, 308, 381, 161, 359, 127, 165, 224, 25, 336, 469, 293, 349, 356, 7, 319, 418, 234, 146, 340, 211, 32, 63, 317, 305, 204, 299, 240, 360, 1, 487, 249, 92, 407, 147
9	10, 52, 14, 55, 25, 15	18, 6, 111, 103, 125, 8, 79, 74, 68, 58, 16, 1	0, 128, 127, 80, 118, 168, 9, 72, 10, 114, 161, 149, 134, 131, 217, 107, 192, 176, 105, 97, 53, 214, 143, 170, 19	381, 202, 428, 184, 264, 312, 504, 133, 138, 257, 119, 364, 272, 66, 232, 342, 359, 124, 161, 127, 165, 308, 224, 336, 25, 469, 293, 349, 356, 7, 319, 418, 234, 340, 146, 211, 32, 317, 63, 305, 204, 299, 240, 360, 1, 487, 249, 92, 407, 170, 246

Table 4: Sensitive neurons on 10 targeted adversarial example sets in *conv13* and *fc* layer of VGG-16 on CIFAR-10.

Target Label	conv13	fc
0	387, 220, 414, 212, 362, 8, 2, 511, 431, 440, 324, 33, 291, 54, 461, 9, 478, 67, 280, 60, 374, 143, 480, 188, 462, 364, 219, 162, 381, 226, 114, 370, 46, 16, 389, 256, 115, 140, 287, 179, 124, 176, 506, 152, 371, 353, 167, 84, 459, 209	0, 1, 6, 8, 9, 5, 7, 3, 4, 2
1	84, 462, 256, 431, 105, 283, 341, 410, 79, 108, 465, 371, 403, 138, 147, 45, 125, 124, 123, 184, 353, 175, 136, 445, 372, 328, 225, 385, 257, 221, 85, 327, 485, 440, 274, 167, 407, 305, 340, 347, 483, 325, 212, 383, 392, 486, 460, 240, 334, 269	1, 8, 4, 9, 7, 6, 2, 5, 3, 0
2	389, 334, 462, 490, 420, 442, 466, 65, 344, 257, 468, 145, 72, 407, 265, 162, 318, 288, 267, 146, 347, 511, 122, 351, 179, 88, 365, 161, 186, 460, 371, 383, 409, 359, 82, 2, 25, 435, 54, 185, 445, 78, 17, 489, 294, 51, 361, 222, 493, 190, 68	2, 8, 1, 9, 0, 3, 7, 6, 4, 5
3	462, 140, 64, 36, 161, 485, 209, 392, 327, 102, 320, 162, 55, 368, 191, 423, 409, 84, 309, 391, 330, 435, 7, 307, 467, 486, 426, 175, 492, 493, 2, 484, 427, 79, 371, 34, 201, 389, 344, 411, 263, 498, 5, 273, 288, 85, 185, 359, 10, 361	3, 1, 8, 9, 4, 0, 7, 6, 5, 2
4	179, 431, 372, 315, 340, 385, 419, 149, 364, 221, 409, 263, 462, 487, 485, 496, 353, 219, 129, 448, 490, 185, 162, 509, 302, 79, 274, 327, 138, 156, 481, 278, 44, 277, 203, 139, 145, 404, 362, 15, 394, 39, 399, 428, 208, 479, 95, 239, 288, 77	4, 1, 9, 8, 7, 2, 3, 6, 5, 0
5	384, 84, 466, 291, 335, 371, 33, 353, 394, 191, 490, 354, 209, 309, 123, 359, 67, 203, 101, 186, 72, 269, 187, 460, 179, 286, 134, 483, 221, 279, 34, 362, 372, 333, 481, 387, 283, 325, 392, 61, 440, 287, 272, 85, 25, 462, 97, 267, 364, 504	5, 1, 6, 4, 9, 2, 8, 0, 7, 3
6	340, 283, 372, 188, 460, 15, 108, 288, 155, 487, 107, 262, 496, 334, 182, 77, 500, 332, 353, 162, 282, 149, 378, 485, 185, 17, 201, 389, 291, 498, 393, 407, 431, 511, 399, 482, 417, 74, 101, 440, 428, 468, 272, 307, 381, 219, 36, 257, 256, 38	6, 1, 9, 7, 0, 8, 4, 2, 3, 5
7	283, 155, 274, 353, 407, 361, 451, 374, 291, 421, 143, 201, 33, 493, 340, 378, 307, 431, 139, 263, 326, 107, 371, 267, 348, 186, 269, 262, 158, 36, 5, 248, 118, 72, 51, 20, 65, 223, 179, 100, 59, 209, 447, 286, 299, 394, 434, 77, 206, 92, 204	7, 8, 1, 6, 9, 0, 4, 2, 5, 3
8	107, 145, 131, 26, 424, 374, 354, 261, 101, 419, 361, 499, 154, 151, 189, 362, 385, 340, 373, 67, 49, 2, 411, 170, 347, 59, 335, 5, 70, 283, 110, 497, 229, 414, 343, 14, 380, 119, 190, 232, 417, 383, 351, 398, 384, 55, 294, 392, 370, 271, 446	8, 4, 5, 1, 7, 9, 2, 6, 3, 0
9	281, 353, 164, 43, 127, 295, 509, 335, 340, 372, 137, 463, 203, 33, 175, 325, 179, 147, 138, 459, 454, 371, 91, 28, 490, 126, 272, 166, 208, 493, 381, 220, 141, 468, 196, 59, 411, 249, 274, 61, 431, 460, 266, 55, 256, 174, 369, 419, 417, 511	9, 4, 1, 6, 2, 5, 8, 7, 3, 0